ABSTRACT

Important material properties of dielectric oxide films fabricated by aqueous chemical solution deposition, such as crystallization, topography, contamination and interfacial layer were evaluated and related to the films' dielectric properties.

Functional ultrathin films (<20 nm thickness) of zirconia, barium zirconate and strontium niobate were deposited. These films were all subjected to the same pyrolysis treatment, based on the high similarity of their precursors' thermal decomposition behavior. The evolution of the chemical purity as a function of temperature and the effect of annealing on the interfacial SiO_2 layer was studied by grazing angle ATR-FTIR. The crystallization behavior was dependent on film thickness and composition as shown by high temperature XRD. C-V characterization demonstrated a k-value in the same order of magnitude as for the ZrO_2 reference material. This is lower than the bulk material's value, thus leaving room for further optimization of the current materials or alternatively selection of other material compositions.

INTRODUCTION

The issue of SiO_x replacement by a high-k material for use as a CMOS gate dielectric that was faced by the electronics industry has been adequately solved by substitution of the traditional SiOx by SiON and more recently by Hf based materials. These materials, however, are only useful for a limited period of time in the ITRS roadmap and will need to be replaced as well, by materials with an even higher k value. Besides the high dielectric constant, these materials should also fulfill specific requirements concerning band gap, leakage current, thermodynamic stability, etc. In order to identify a suitable material composition, we are studying films in the thickness range of the final application (< 20 nm) fabricated by aqueous chemical solution deposition [1]. CSD is commonly applied for the deposition of electronic metal oxide films, with thicknesses well above 100 nm and applications such as non-volatile memory, M(N)EMS, electrodes,…. The deposition of thin films < 20 nm is unusual, as it is commonly believed that below a few tens of nanometers uniform films cannot be obtained. However, we showed that this uncomplicated technique based on spin-coating of aqueous precursor solutions followed by a thermal treatment, was capable of ultrathin film deposition onto SiOx/Si substrates [2]. Film thicknesses down to less than 5 nm were used for fabrication of functional MOS devices with good dielectric quality, fit for k-value and leakage behavior assessment after optimization of the precursor and thermal treatment [3].

The future generation of high-k dielectrics is sought in ternary metal oxides (MM'O_x). Due to the more complex composition compared to binary oxides, their synthesis can be complicated e.g. by the possibility of phase segregation. However, the CSD process starts from multimetal ion precursor sol(ution)s, allowing a high degree of homogeneity [4]. Therefore, it is expected to allow relatively low temperature phase formation and to be ideal for the preparation of multimetal oxides. Aqueous CSD, starting from aqueous solutions of metal ions stabilized by electron donating ligands such as hydrogen peroxide and citric acid, has the supplemental advantage of cost effectiveness and avoids harmful solvents used in alcoholic sol-gel routes [5].

Here the aqueous CSD of ultrathin barium zirconate and strontium niobate films will be presented. The dielectric and material properties will be compared to zirconium oxide, used here as a well characterized reference material.

EXPERIMENT

Aqueous precursor solutions were prepared for the different material compositions under study, by a method similar to previous reports [6-8]. The exact concentration was determined by ICP-AES (Optima 3000, Perkin Elmer). Gels were obtained by evaporation of the precursor

solutions (air-flushed laboratory furnace, 60°C) and their thermograms were recorded on a TGA 2950 (TA Instruments) in flowing dry air. The solutions were diluted to obtain concentrations (0.01 – 0.1 mol L^{-1}) suitable for deposition of the desired oxide film thicknesses (< 30 nm). Films were deposited using an SPS Polos spin-coater (3000 rpm, 30s). Thermal treatment was carried out stepwise on hot plates in ambient air and the films were finally annealed (FA) in a tube furnace (0.5 L min^{-1} dry air). Film thicknesses were determined by single wavelength ellipsometry (Plasmos), calibrated by XRR (D8 Bruker). Grazing angle ATR-FTIR spectra were obtained using a Harrick GATR accessory (65° incident angle, Ge hemispherical crystal) on a Bruker Vertex 70 FTIR spectrometer. In-situ high-temperature XRD patterns were recorded on a Bruker D8 with an Anton Paar HTK 1200 chamber and a position sensitive detector spanning a range of 4°2θ (30°C/min, static air). SEM images were recorded on a FEI Quanta 200FEG and tapping mode AFM was carried out on a Veeco AFM with an etched Si probe. C-V characteristics were measured on evaporated Pt dots (~1.10^{-4} – 8.10^{-4} cm^2) with a Keithley 4200 tester. Forming gas anneal (5% H$_2$ / 95% N$_2$) was carried out at 520°C, 20 min.

RESULTS AND DISCUSSION

During the CSD process, precursor films are obtained by spin-coating. An appropriate thermal treatment is needed to convert the precursor to the oxide, and is selected based on the thermal behavior of the bulk precursor. Thermograms of precursor gels for zirconia, strontium niobate and barium zirconate (citric acid : metal ion = 4:1) are shown in *Figure 1*.
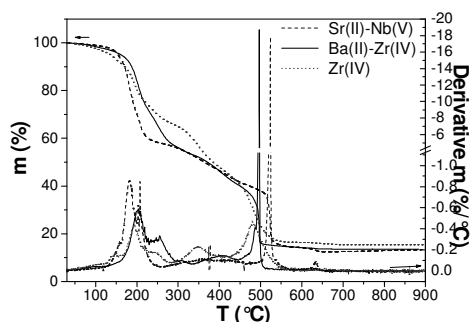
Figure 1 TGA of precursor gels (10°C/min, 100 ml/min dry air)

This illustrates the typical decomposition behavior of the gels, which is characterized by three major steps around 200-250°C, 350-400°C and 480-550°C. The thermal decomposition is finished between 600-650°C. Based on this bulk gel behavior, the drying and pyrolysis steps of the thin films were chosen at 260°C/2' and 480°C/2', followed by a final anneal applied as a densification or crystallization step at higher temperatures (between 600°C and 900°C).

The behavior of the precursor films might differ from the bulk behavior due to the volume effects as well as the influence of the substrate. Therefore, the evolution of the precursor film's chemical structure during the heat treatment was studied off-line by GATR-FTIR, as illustrated for a Zr(IV) precursor film in Figure 2a. The spindried film clearly shows the presence of carboxylate groups with vibrations around 1400 and 1600 cm^{-1} (symmetric and asymmetric stretching of –COO$^-$) as well as –COOH vibrations at 1720 cm^{-1} [9]. The free acid is decomposed at relatively low temperatures (260°C), while the vibrations at 1400 and 1600 cm^{-1} remain up to 480°C due to the higher temperature stability of the citrato-complex. The formation of amides, which are thermostable as well, also leads to vibrations in this wavenumber region. After heat treatment up to 480°C a strong increase of the absorbance is observed at ~700 cm^{-1}, which indicates oxide formation. The band is broad, which is ascribed to a limited crystallinity at this low temperature. Annealing at higher temperatures of 600-800°C leads to sharpening of the band at 700 cm^{-1}, related with further crystallization and to disappearance of the organic rest

fraction (1400-1600 cm^{-1}). The silicon oxide bands at 1250 and 1050 cm^{-1} intensify significantly after annealing at 800°C, which is ascribed to further oxidation of the substrate.

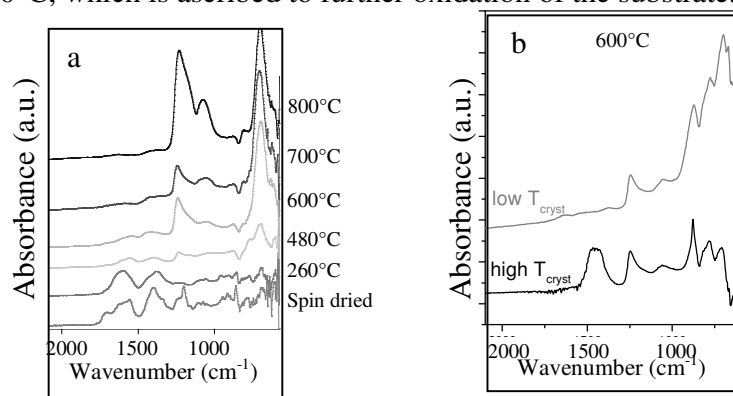*Figure 2 GATR-FTIR of a) Zr(IV) film heat treated at different temperatures and b) Sr(II)-Nb(V) compositions (low T$_{cryst}$ Sr:Nb 1:2, high T$_{cryst}$ Sr:Nb 2:1) annealed at 600°C/30' in dry air*

For the Zr(IV) precursor film, no carbonate formation was detected in the film during decomposition. This is not the case for the Ba(II)-Zr(IV) precursor film: it showed the presence of a persistent carbonate phase, only removed by annealing at high temperature (800°C). For Sr(II)-Nb(V) the presence of a carbonate phase (CO$_3^{2-}$ ~1500 cm^{-1}) was either observed or not depending on the ratio of Sr : Nb (*Figure 2*b). The formation of alkaline earth carbonates during the thermal decomposition of organic precursor gels is well known. Even though these carbonates have very high decomposition temperatures, the decomposition can be energetically favoured by the competitive multimetal oxide formation. This explains the relatively low decomposition temperature observed for BaCO$_3$ (only 800°C) and the difference between the different Sr : Nb compositions, which form different oxide phases. For a Sr:Nb 1:2 composition with the lowest crystallization temperature, no carbonate was detected even at a temperature as low as 600°C.

From the GATR-FTIR an indication for the crystallization of the films can be obtained, besides the chemical structural information, as discussed above. However, in-situ measurement by HT-XRD allows direct study of the crystallization of the films. This behavior is compared with the crystallization of the gel powder in Figure 3.
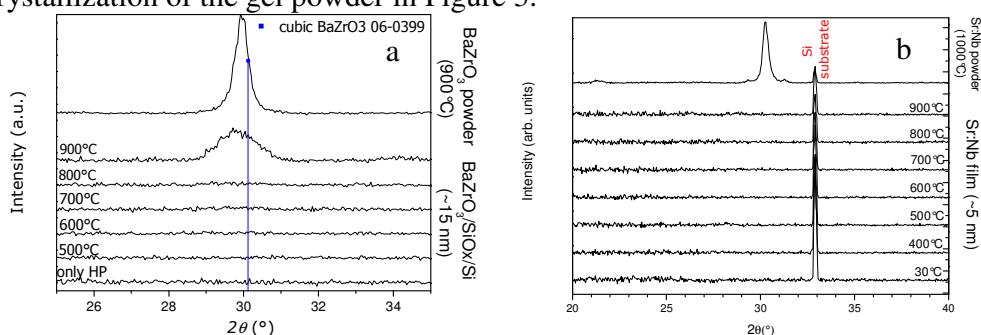

Figure 3 HT-XRD of a) a barium zirconate and b) a strontium niobate precursor film compared to the powder of the same composition

Ba(II)-Zr(IV) precursor films with t~15 nm (after anneal at 600°C), showed crystallization of cubic BaZrO$_3$ between 800 and 900°C (Figure 3a). The peak width is high, indicating nanocrystallinity. For the precursor gel however, BaZrO$_3$ powder crystallized between 600 and 700°C already. It is concluded that the volume of the precursor material which is heat treated and/or the substrate has an effect on the observed crystallization temperature, in

accordance with literature [10]. An even thinner film of strontium niobate (Sr/Nb=2/1, t~5 nm after anneal at 600°C) was not observed to crystallize at all, even though the crystallization of the gel yielded the desired crystal phase (Figure 3b). The ratio of Sr:Nb metal ions in the composition determines which crystal phase is favoured and thus the crystallization energy. In this way, a crystallization temperature dependence from the composition can be expected also.

To show that this lack of crystallization is not explained by the detection limit of the diffractometer for the 5 nm thick film, off-line XRD patterns of ZrO_2 films of a similar thickness are shown in Figure 4a.
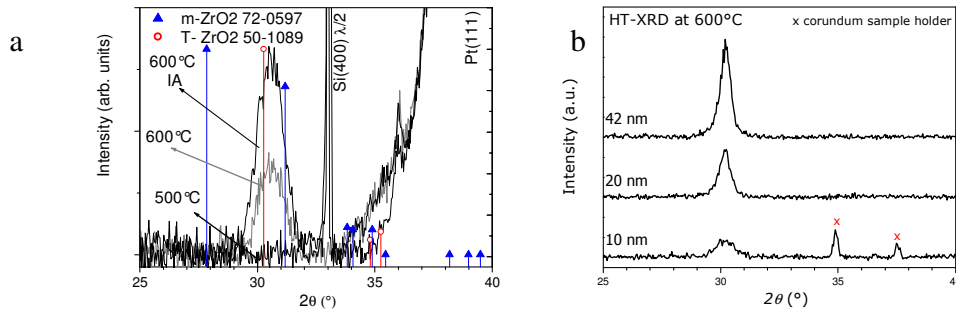

Figure 4 a) Room temperature XRD of ZrO$_2$/Pt films (~5 nm) 500°C, 600°C, 600°C IA compared to b) HT-XRD at 600°C for ZrO$_2$/SiO$_x$ films of different thickness from ellipsometry

Crystallization of the tetragonal phase was clearly observed after annealing at 600°C. Note that intermediate annealing (IA) of each individual layer at 600°C leads to an increased crystallinity. The films in Figure 4a were deposited on platinized silicon, but the effect of the substrate is insignificant here: ZrO_2 films annealed at 600°C on SiO_x/Si also showed crystallization at relatively low temperature for different thicknesses (Figure 4b).

The resistance against crystallization up to high temperatures can be considered as an advantage to obtain high interface quality, and to suppress leakage currents and dopant diffusion along grain boundaries [11]. On the other hand, crystalline phases may be required to obtain a sufficiently high *k* value, although certain theoretical predictions point the other way [12].

To verify the uniformity of the CSD deposited ultrathin films, the topography after anneal at 600°C and 700°C was studied for different material compositions (Figure 5). For the ZrO_2 reference material smooth surfaces were obtained, as demonstrated in SEM and AFM (Figure 5a and b). Note that at the annealing temperatures used here (600 and 700°C) the ZrO_2 is crystallized as the tetragonal phase, at least partially. The strontium niobate on the other hand shows a much higher roughness already at 600°C (Figure 5c), where it is not crystallized yet. After annealing at 700°C this specific composition and thickness (Sr:Nb 1:2, ~20nm) showed significant crystallization. This strongly affects the topography by the formation of large, elongated grains (Figure 5d) and leads to a much higher roughness.
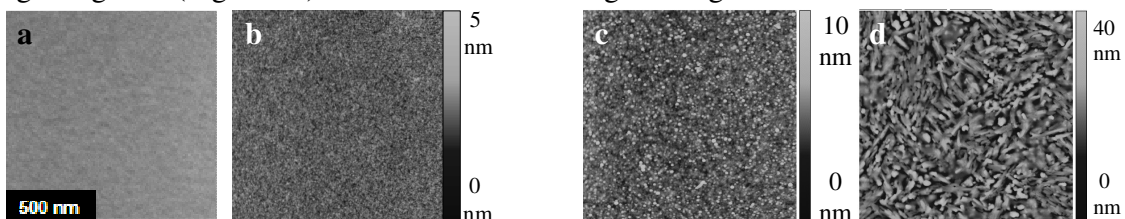

*Figure 5 a) SEM of ZrO$_2$ with FA at 600°C (t~10 nm) and 2*2 µm^2 AFM height images of b) ZrO$_2$ with FA at 700°C and a strontium niobate (t~20 nm) with FA at c) 600°C and d) 700°C*

The C-V behavior of the different metal oxides studied here is illustrated in Figure 6 (FA 600°C/30 min). A large negative flatband voltage shift was observed for the multimetal oxides. For barium zirconate |V$_{FB}$| showed a large increase as a function of thickness, indicating positive

charges in the bulk of the layer. The capacitances obtained for barium zirconate and strontium niobate are in the same order of magnitude as for ZrO_2. These correspond to lower than expected k-values (~15 for barium zirconate, ~19 for strontium niobate, extracted from thickness series not shown here) compared to bulk material and thick film properties [13, 14]. This can be explained by thickness effects [15], the amorphous character and possible interfacial reactions on SiO_x/Si substrates [11] and thus leaves room for optimization in the deposition process.
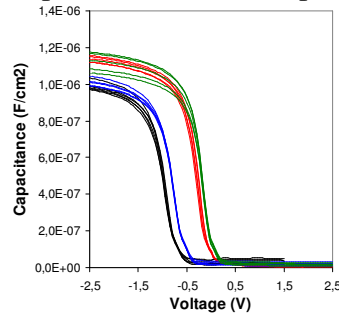

Figure 6 C-V curves of a barium zirconate (black), two strontium niobate compositions (green, blue) and a zirconia (red) thin film (t ~ 6-8 nm)

CONCLUSIONS

Aqueous CSD was applied as a flexible deposition method for ultrathin multimetal oxide films with different compositions and possible application as high-k dielectrics. Assessment of these materials' properties such as their chemical purity, crystallization behavior and microstructural features, allows the development of a knowledge-basis to support understanding and improvement of the film's dielectric properties. Though the films studied here showed relatively high-k values compared to SiO_2, further study is necessary for the identification of a suitable "super"high-k material to replace the Hf based materials which are currently commercially in use. Because of its advantages for multimetal oxide synthesis and its high speed through simple instrumentation, aqueous CSD will continu to be used for this prospection goal.

ACKNOWLEDGEMENTS

REFERENCES

1. A. Hardy, M.K. Van Bael, J. D'Haen, O. Douhéret, M. D'Olieslaeger, J. Mullens, S. Van Elshocht, S. De Gendt, C. Adelmann, M. Caymax, T. Conard, T. Witters, H. Bender, O. Richard and M. Heyns, *J. Mater. Res.* **22**, 3484 (2007).
2. S. Van Elshocht, A. Hardy, T. Witters, C. Adelmann, M. Caymax, T. Conard, S. De Gendt, A. Franquet, M. Heyns, M.K. Van Bael and J. Mullens, *Electrochem. Solid State Lett.* **10**, G15 (2007).
3. S. Van Elshocht, A. Hardy, C. Adelmann, M. Caymax, T. Conard, A. Franquet, O. Richard, M.K. Van Bael, J. Mullens and S. De Gendt, *J. Electrochem. Soc.* **155 (4)**, in press (2008).
4. R.W. Schwartz, T. Schneller and R. Waser, *C. R. Chim.* **7**, 433 (2004).
5. H. Van den Rul, M.K. Van Bael, A. Hardy, K. Van Werde and J. Mullens In *Handbook of Nanoceramics and Their Based Nanodevices*; H. S. Nalwa, T. Y. Tseng, Eds., (in press, 2008).

6. K. Van Werde, G. Vanhoyland, D. Nelis, D. Mondelaers, M.K. Van Bael, J. Mullens and L.C. Van Poucke, *J. Mater. Chem.* **11**, 1192 (2001).
7. D. Nelis, K. Van Werde, D. Mondelaers, G. Vanhoyland, H. Van den Rul, M.K. Van Bael, J. Mullens and L.C. Van Poucke, *J. Sol-Gel Sci. Technol.* **26**, 1125 (2003).
8. K. Van Werde, G. Vanhoyland, D. Mondelaers, H. Van den Rul, M. Van Bael, J. Mullens and L. Van Poucke, *J. Mater. Sci.* **42**, 624 (2007).
9. K. Nakamoto *Infrared and Raman Spectra of Inorganic and Coordination Compounds Part B: Applications in Coordination, Organometallic, and Bioinorganic Chemistry*, 5th edition ed.; John Wiley & Sons, Inc.: New York, (1997).
10. C. Zhao, G. Roebben, M. Heyns and O. van der Biest, *Euro Ceramics Vii, Pt 1-3 Key Eng. Mater.* **206-2**, 1285 (2002).
11. J. Robertson, *Rep. Prog. Phys.* **69**, 327 (2006).
12. P. Delugas, V. Fiorentini, A. Filippetti and G. Pourtois, *Phys. Rev. B* **76**, 104112 (2007).
13. H. Stetson and B. Schwartz, *J. Am. Ceram. Soc.* **44**, 420 (1961).
14. I. Levin, J.Y. Chan, J.H. Scott, L. Farber, T.A. Vanderah and J.E. Maslar, *J. Solid State Chem.* **166**, 24 (2002).
15. M. Stengel and N.A. Spaldin, *Nature* **443**, 679 (2006).